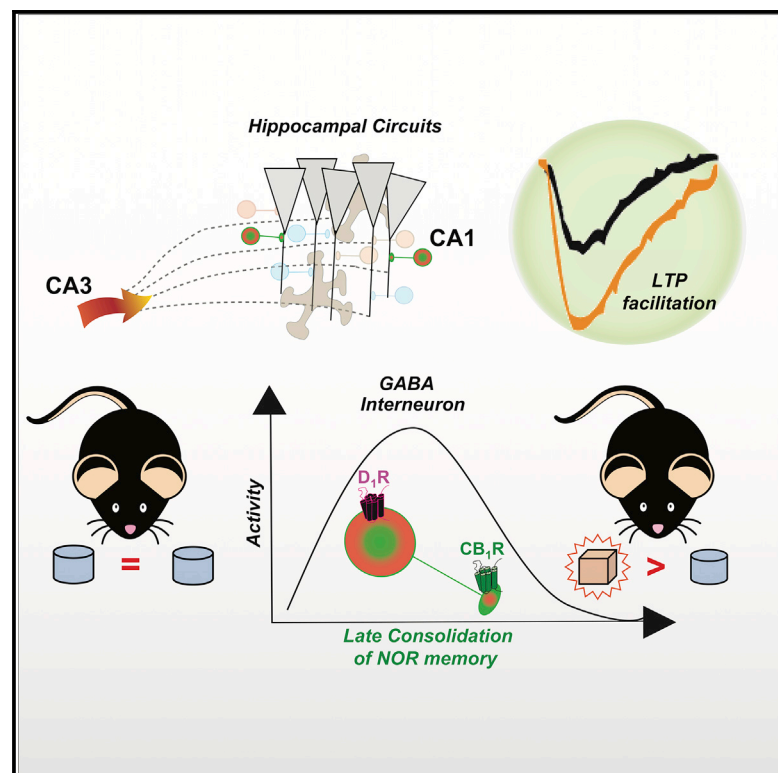


# Specific Hippocampal Interneurons Shape Consolidation of Recognition Memory

## Graphical Abstract



## Authors

Jose F. Oliveira da Cruz,  
 Arnau Busquets-Garcia, Zhe Zhao, ...,  
 Filippo Drago, Giovanni Marsicano,  
 Edgar Soria-Gómez

## Correspondence

giovanni.marsicano@inserm.fr (G.M.),  
 edgarjesus.soria@ehu.eus (E.S.-G.)

## In Brief

Oliveira da Cruz et al. show that a specific subpopulation of hippocampal CB<sub>1</sub> and D<sub>1</sub> receptor-positive neurons controls late consolidation of recognition memory and associated synaptic plasticity by moderating local inhibitory GABAergic activity in the hippocampus.

## Highlights

- CB<sub>1</sub>Rs are present in hippocampal D<sub>1</sub>R-positive interneurons
- CB<sub>1</sub>R/D<sub>1</sub>R-positive interneurons control the late phase of recognition memory
- CB<sub>1</sub>R/D<sub>1</sub>R-positive interneurons control learning-induced facilitation of LTP



## Report

# Specific Hippocampal Interneurons Shape Consolidation of Recognition Memory

Jose F. Oliveira da Cruz,<sup>1,2,3,9</sup> Arnau Busquets-Garcia,<sup>1,2,4,9</sup> Zhe Zhao,<sup>1</sup> Marjorie Varilh,<sup>1,2</sup> Gianluca Lavanco,<sup>1,2,5</sup> Luigi Bellocchio,<sup>1,2</sup> Laurie Robin,<sup>1</sup> Astrid Cannich,<sup>1,2</sup> Francisca Julio-Kalajzić,<sup>1,2</sup> Thierry Lesté-Lasserre,<sup>1,2</sup> Marlène Maitre,<sup>1,2</sup> Filippo Drago,<sup>4</sup> Giovanni Marsicano,<sup>1,2,10,11,\*</sup> and Edgar Soria-Gómez<sup>1,2,6,7,8,10,\*</sup>

<sup>1</sup>INSERM U1215, NeuroCentre Magendie, Bordeaux 33300, France

<sup>2</sup>University of Bordeaux, Bordeaux 33300, France

<sup>3</sup>New York University, Center for Neural Science, New York, NY 10003, USA

<sup>4</sup>Integrative Pharmacology and System Neuroscience, IMIM-Hospital del Mar Medical Research Institute, Barcelona 08003, Spain

<sup>5</sup>Department of Biomedical and Biotechnological Sciences, Section of Pharmacology, University of Catania, Catania 95124, Italy

<sup>6</sup>Ikerbasque-Basque Foundation for Science, Bilbao 48013, Spain

<sup>7</sup>Department of Neuroscience, Faculty of Medicine and Nursing, University of the Basque Country (UPV/EHU) Leioa 48940, Spain

<sup>8</sup>Achucarro Basque Center for Neuroscience, Leioa 48940, Spain

<sup>9</sup>These authors contributed equally

<sup>10</sup>Senior author

<sup>11</sup>Lead Contact

\*Correspondence: [giovanni.marsicano@inserm.fr](mailto:giovanni.marsicano@inserm.fr) (G.M.), [edgarjesus.soria@ehu.eus](mailto:edgarjesus.soria@ehu.eus) (E.S.-G.)

<https://doi.org/10.1016/j.celrep.2020.108046>

## SUMMARY

A complex array of inhibitory interneurons tightly controls hippocampal activity, but how such diversity specifically affects memory processes is not well understood. We find that a small subclass of type 1 cannabinoid receptor (CB<sub>1</sub>R)-expressing hippocampal interneurons determines episodic-like memory consolidation by linking dopamine D<sub>1</sub> receptor (D<sub>1</sub>R) signaling to GABAergic transmission. Mice lacking CB<sub>1</sub>R<sub>s</sub> in D<sub>1</sub>-positive cells (D<sub>1</sub>-CB<sub>1</sub>-KO) display impairment in long-term, but not short-term, novel object recognition memory (NOR). Re-expression of CB<sub>1</sub>R<sub>s</sub> in hippocampal D<sub>1</sub>R-positive cells rescues this NOR deficit. Learning induces an enhancement of *in vivo* hippocampal long-term potentiation (LTP), which is absent in mutant mice. CB<sub>1</sub>R-mediated NOR and the associated LTP facilitation involve local control of GABAergic inhibition in a D<sub>1</sub>-dependent manner.

This study reveals that hippocampal CB<sub>1</sub>R-/D<sub>1</sub>R-expressing interneurons control NOR memory, identifying a mechanism linking the diversity of hippocampal interneurons to specific behavioral outcomes.

## INTRODUCTION

Formation of episodic memory is a multistep brain process that requires activity of the medial temporal lobe (Squire et al., 2007). The hippocampus in particular participates in long-term storage of recently acquired events. Hippocampal circuits are regulated by a large variety of local inhibitory interneurons that are controlled by neuromodulatory systems ensuring their coordinated function to shape behavioral responses (Klausberger and Somogyi, 2008); the identities and functions of the interneurons are under intense scrutiny (Harris et al., 2018; Pelkey et al., 2017; Parra et al., 1998).

The endocannabinoid system is a brain-modulatory signaling hub formed mainly by type 1 cannabinoid receptors (CB<sub>1</sub>R<sub>s</sub>), their endogenous ligands (endocannabinoids), and enzymes for their synthesis and degradation. In the hippocampus, CB<sub>1</sub>R<sub>s</sub> are present in principal neurons and astroglial cells (Busquets-Garcia et al., 2015; Oliveira da Cruz et al., 2016). However, the largest expression of CB<sub>1</sub>R<sub>s</sub> resides in GABAergic interneurons (Marsicano and Kuner, 2008; Katona and Freund, 2012),

where they modulate local inhibition of hippocampal circuits. Particularly, the largest amount of CB<sub>1</sub>R<sub>s</sub> is expressed in cholecystokinin (CCK)-positive interneurons, which are characterized by asynchronous neurotransmitter release (Harris et al., 2018; Katona et al., 1999; Marsicano and Lutz, 1999).

Hippocampal CB<sub>1</sub>R<sub>s</sub> control episodic-like memory processes and synaptic plasticity (Robin et al., 2018; Hebert-Chatelain et al., 2016; Puighermanal et al., 2009). However, the specific locations where these receptors participate in the mechanisms underlying hippocampus-dependent memory are only partially known.

Activity-dependent long-term changes in hippocampal synaptic transmission are considered cellular correlates of memory consolidation (Nicoll, 2017; Whitlock et al., 2006), which involves local dopamine D<sub>1</sub> receptor (D<sub>1</sub>R) signaling (Lisman et al., 2011; Yamasaki and Takeuchi, 2017). Exposure to hippocampus-dependent behavioral tasks induces changes in long-term potentiation (LTP) of synaptic transmission that require activation of D<sub>1</sub>-like receptors (Frey et al., 1990; Granado et al., 2008; Li et al., 2003; Lemon and Manahan-Vaughan, 2006). A



novel subpopulation of hippocampal CB<sub>1</sub>R/CCK-positive interneurons containing D<sub>1</sub>R was recently described (Puighermanal et al., 2017; Gangarossa et al., 2012). However, the potential interactions between D<sub>1</sub>R and CB<sub>1</sub>R in regulating learning-induced plasticity, activity of hippocampal circuits, and memory processes remain unexplored.

Here we assessed the role of D<sub>1</sub>R/CB<sub>1</sub>R-positive cells in regulation of episodic-like novel object recognition (NOR) memory. We found that conditional deletion of the CB<sub>1</sub>R gene in hippocampal D<sub>1</sub>R-positive cells impairs long- but not short-term NOR memory and learning-induced LTP enhancement involving local control of GABAergic transmission. These intriguing results suggest that CB<sub>1</sub>R signaling provides a functional link between hippocampal dopaminergic and GABAergic control of synaptic plasticity and memory consolidation.

## RESULTS

### CB<sub>1</sub>Rs in Hippocampal D<sub>1</sub>R-Positive Neurons Are Necessary for Consolidation of NOR Memory

Mutant mice bearing a deletion of the CB<sub>1</sub>R gene in cells expressing D<sub>1</sub>R (D<sub>1</sub>-CB<sub>1</sub>-knockout [KO] mice; Monory et al., 2007) displayed no phenotype in the short-term version (3 h post-training) of a NOR task (Figures 1A and 1B; Puighermanal et al., 2009; Busquets-Garcia et al., 2011; Robin et al., 2018). Conversely, they showed strong impairment in long-term (24 h) memory compared with their wild-type (WT) littermates (Figure 1C), with no changes in total exploration time (Figures S1A–S1D).

The majority of CB<sub>1</sub>Rs in D<sub>1</sub>R-positive neurons have been characterized previously in striatonigral circuits (Monory et al., 2007). Considering the involvement of these circuits in NOR memory (Darvas and Palmiter, 2009), we tested the role of striatal CB<sub>1</sub>Rs. We infused an adeno-associated virus carrying a Cre-dependent expression of CB<sub>1</sub>Rs (pAAV-CAG-DIO-CB<sub>1</sub>) into the striatum of D<sub>1</sub>-CB<sub>1</sub>-KO mice to obtain re-expression (RS) of CB<sub>1</sub>Rs in cells where Cre is present (hereafter called D<sub>1</sub>R-positive) in this brain region (striatum [STR]-CB<sub>1</sub>-RS mice; Figures 1D and 1E), as revealed by immunodetection of a myc-tagged version of CB<sub>1</sub>Rs (CB<sub>1</sub>R-myc; STAR Methods; Figure 1E). This re-expression was not sufficient to rescue the phenotype of D<sub>1</sub>-CB<sub>1</sub>-KO mice in long-term NOR (Figures 1F, S1E, and S1F), suggesting that CB<sub>1</sub>Rs in striatal D<sub>1</sub>R-positive cells do not participate in this type of memory. Anatomical data indicate that a subset of hippocampal neurons contain D<sub>1</sub>Rs (Gangarossa et al., 2012), likely co-expressing CB<sub>1</sub>R protein (Puighermanal et al., 2017). Thus, we re-express the CB<sub>1</sub>R gene in the hippocampus of D<sub>1</sub>-CB<sub>1</sub>-KO mice to obtain hippocampus (HPC)-CB<sub>1</sub>-RS mice (Figures 1D and 1G). This manipulation fully rescued the phenotype of the mutant mice (Figure 1F, S1E, and S1F), indicating that hippocampal CB<sub>1</sub>Rs expressed in D<sub>1</sub>R-positive cells are required for NOR memory.

We recently reported that deletion of CB<sub>1</sub>Rs in hippocampal glial acidic fibrillary protein (GFAP)-positive cells (i.e., mainly astrocytes, GFAP-CB<sub>1</sub>-KO mice) also impaired NOR memory (Robin et al., 2018). Indeed, GFAP-CB<sub>1</sub>-KO mice were impaired in NOR (Figures S1G–S1I; Robin et al., 2018), but, in contrast to D<sub>1</sub>-CB<sub>1</sub>-KO mice, this phenotype extended to short-term NOR

memory (Figures S1J–S1L). This difference suggests that CB<sub>1</sub>Rs expressed in hippocampal astrocytes or D<sub>1</sub>R-positive cells might control distinct phases of NOR memory consolidation.

The primary function of CB<sub>1</sub>R activation in neurons is to decrease neurotransmitter release (Castillo et al., 2012; Busquets-Garcia et al., 2017). Accordingly, deletion of CB<sub>1</sub>Rs from neurons often results in excessive neurotransmission. Thus, we reasoned that inhibition of hippocampal D<sub>1</sub>R-positive neurons during NOR consolidation should be able to rescue the memory impairment of D<sub>1</sub>-CB<sub>1</sub>-KO mice. Viral vectors carrying Cre-dependent expression of an inhibitory designer receptor exclusively activated by designer drugs (DIO-hM4DGi, Gi-DREADD; Robinson and Adelman, 2015) or control mCherry protein were infused into the hippocampi of D<sub>1</sub>-CB<sub>1</sub>-KO mice and WT littermates (Figure 1H). Post-training clozapine N-oxide (CNO) injections did not affect the NOR performance of D<sub>1</sub>-CB<sub>1</sub>-KO and WT mice injected with Gi-DREADD or mCherry, indicating that the drug or its metabolites had no effect per se (Gomez et al., 2017; Figures 1I, S1M, and S1N). Conversely, post-acquisition CNO treatment fully rescued the NOR impairment of D<sub>1</sub>-CB<sub>1</sub>-KO mice expressing Gi-DREADD (Figures 1I, S1M, and S1N). This strongly suggests that excessive activity of D<sub>1</sub>R-positive neurons during the consolidation process is responsible for the memory impairment observed in D<sub>1</sub>-CB<sub>1</sub>-KO mice.

### CB<sub>1</sub>Rs in Hippocampal D<sub>1</sub>R-Positive Neurons Control Learning-Induced Changes of LTP *In Vivo*

Cellular and molecular mechanisms underlying activity-dependent changes in synaptic plasticity are proposed to underlie long-term memory (Aggleton and Morris, 2018). Previous studies showed that conditional and global deletion of CB<sub>1</sub>Rs in neuronal and glial cell populations induces deficits in learning and associated synaptic plasticity (Busquets-Garcia et al., 2017; Robin et al., 2018). To address the role of CB<sub>1</sub>Rs in hippocampal D<sub>1</sub>R-positive neurons in modulation of synaptic plasticity, we recorded *in-vivo*-evoked field excitatory postsynaptic potentials (fEPSPs) in the hippocampal CA3-CA1 pathway of anesthetized mice. High-frequency stimulation (HFS) induced similar long-lasting LTP of synaptic fEPSPs in D<sub>1</sub>-CB<sub>1</sub>-KO and WT littermates (Figures 2A and 2B), indicating that hippocampal D<sub>1</sub>R/CB<sub>1</sub>R-positive neurons are dispensable for expression of LTP in naive animals.

HPC-dependent memory-related processes such as LTP are sensitive to pharmacological and genetic modulation of hippocampal D<sub>1</sub>Rs, particularly after learning (Li et al., 2003; Lemon and Manahan-Vaughan, 2006; Takeuchi et al., 2016; Yamasaki and Takeuchi, 2017). Thus, we hypothesized that CB<sub>1</sub>Rs in D<sub>1</sub>R-positive neurons may modulate learning-dependent hippocampal synaptic plasticity. To explore whether acquisition of the NOR task modulates *in vivo* LTP, we recorded fEPSPs from C57Bl6/NRj mice after a NOR task (Figure 2C). HFS induced stronger LTP in animals exposed to NOR acquisition than in control mice (Figures 2D and 2E), showing that the training modulates hippocampal synaptic plasticity. Strikingly, D<sub>1</sub>-CB<sub>1</sub>-KO mice lacked this learning-induced enhancement of LTP (Figures 2F and 2G). Thus, physiological activation of CB<sub>1</sub>Rs in

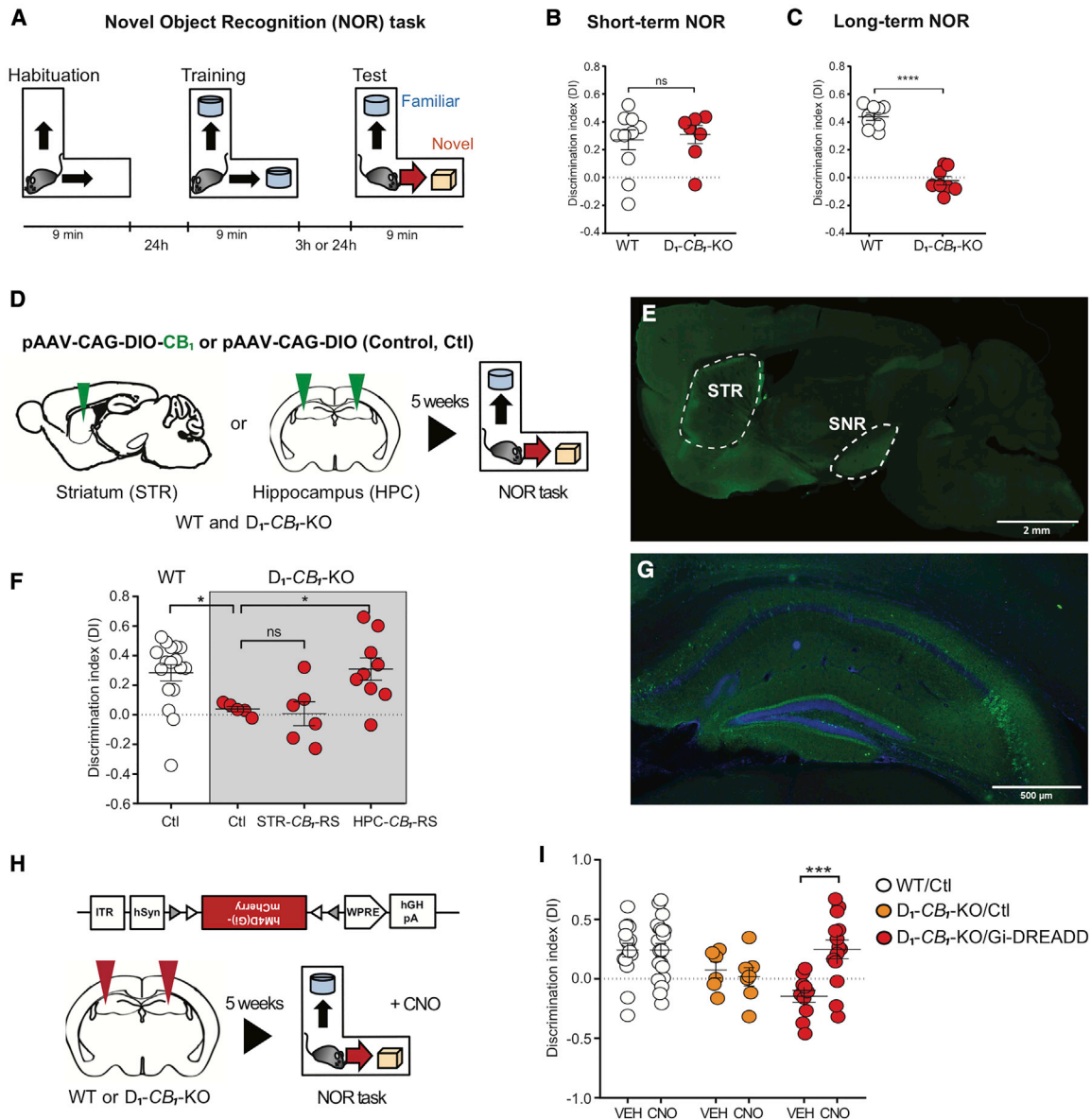


**Figure 1. Hippocampal  $CB_1$ R<sub>s</sub> in  $D_1$ R-Positive Cells Are Necessary for Late but Not Early Consolidation of NOR**

(A) Schematic representation of the NOR memory task.

(B) Short-term (3 h) NOR memory performance of  $D_1-CB_1$ -WT mice ( $n = 10$ ) and  $D_1-CB_1$ -KO littermates ( $n = 7$ ).

(C) Long-term NOR (24 h) memory performance of  $D_1-CB_1$ -WT mice ( $n = 9$ ) and  $D_1-CB_1$ -KO littermates ( $n = 8$ ).

(D) Schematic representation of the experiment using viral re-expression of the  $CB_1$ R gene in the striatum (STR) or the hippocampus (HPC) of  $D_1-CB_1$ -WT mice and  $D_1-CB_1$ -KO littermates.

(E) Representative images of Cre-expressing  $D_1-CB_1$ -KO mice injected with  $CB_1$ R-myc in the STR using the same procedure as described in (D) (STAR Methods). Scale bar, 2 mm.

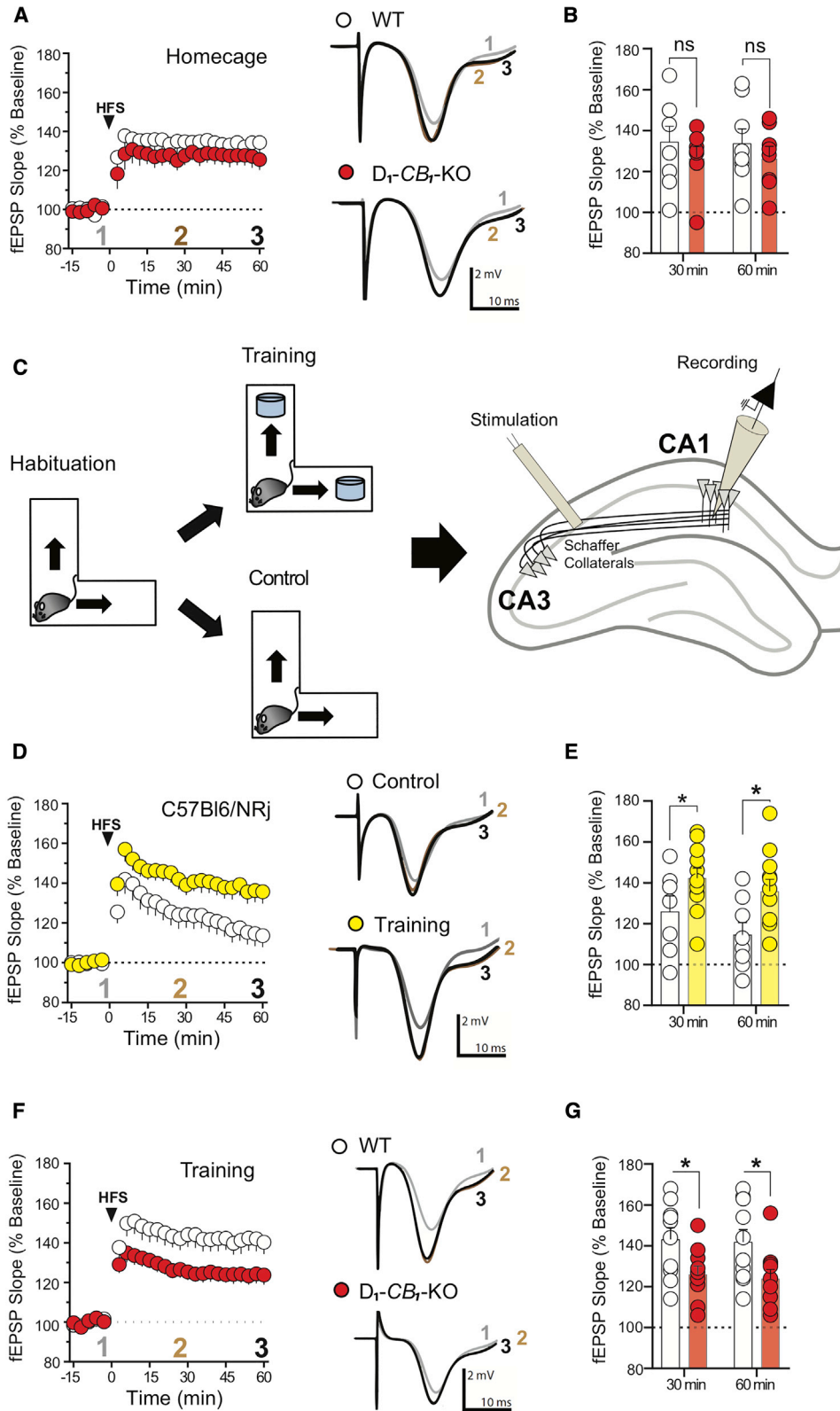
(F) NOR memory performance of mice with re-expression of the  $CB_1$ R gene in the STR or HPC. Control,  $n(D_1-CB_1$ -WT) = 17 and  $n(D_1-CB_1$ -KO) = 5; STR- $CB_1$ -RS,  $n(D_1-CB_1$ -KO) = 6; HPC- $CB_1$ -RS,  $n(D_1-CB_1$ -KO) = 9.

(G) Immunofluorescence of cells expressing  $CB_1$ R-myc in the HPC. Scale bar, 500  $\mu$ m.

(H) Schematic representation of the experiment using viral expression of the Gi-DREADDs or mCherry in the HPC of  $D_1-CB_1$ -WT mice and  $D_1-CB_1$ -KO littermates. Clozapine N-oxide (CNO; 2 mg/kg) injections take place after the training phase of the NOR task.

(I) NOR memory performance of  $D_1-CB_1$ -WT mice injected intra-hippocampally with hM4D(Gi) virus or mCherry ( $n$  VEH = 16,  $n$  CNO = 21),  $D_1-CB_1$ -KO mice injected with mCherry ( $n$  VEH = 6,  $n$  CNO = 7), and  $D_1-CB_1$ -KO mice injected intra-hippocampally with hM4D(Gi) ( $n$  VEH = 11,  $n$  CNO = 14).

Data, mean  $\pm$  SEM. \* $p < 0.05$ , \*\*\* $p < 0.001$ , \*\*\*\* $p < 0.0001$ . ns, not significant. See also Figure S1 and Table S1.



(legend on next page)

hippocampal D<sub>1</sub>R-positive neurons is required for learning-dependent facilitation of LTP.

### CB<sub>1</sub>R in Hippocampal D<sub>1</sub>R-Positive Neurons Modulate NOR Memory Consolidation through a GABA-Dependent Mechanism

D<sub>1</sub>Rs are expressed in different hippocampal cells, including subsets of GABAergic and glutamatergic neurons (Gangarossa et al., 2012). Considering that CB<sub>1</sub>R signaling decreases the activity of hippocampal neurons (Busquets-Garcia et al., 2017; Castillo et al., 2012), we asked whether excessive glutamatergic or GABAergic neurotransmission might underlie the phenotype of D<sub>1</sub>-CB<sub>1</sub>-KO mice. Thus, we injected non-amnesic doses (Puighermanal et al., 2009) of the NMDA receptor blocker MK-801, the AMPA/kainate receptor antagonist NBQX (Figure S2A), or the GABA<sub>A</sub> receptor antagonist bicuculline into D<sub>1</sub>-CB<sub>1</sub>-KO and WT littermates immediately after NOR training. MK-801 and NBQX did not alter memory performance in WT mice, nor did it rescue the amnesic phenotype of D<sub>1</sub>-CB<sub>1</sub>-KO littermates (Figures 3A, S2B, and S2C). Conversely, bicuculline completely reversed the memory impairment of D<sub>1</sub>-CB<sub>1</sub>-KO mice when injected immediately after training or 1 h later without affecting WT littermates' performance (Figures 3A, S2B, and S2C).

These data indicate that excessive GABAergic but not glutamatergic ionotropic receptor activity is involved in the phenotype of D<sub>1</sub>-CB<sub>1</sub>-KO mice. A large proportion of GABAergic hippocampal interneurons contain CB<sub>1</sub>R mRNA, which is expressed at different levels (high CB<sub>1</sub>R- and low CB<sub>1</sub>R-expressing cells; Marsicano and Lutz, 1999). Conversely, D<sub>1</sub>R mRNA is expressed at very low levels in the HPC (<http://mouse.brain-map.org/experiment/show/35>; data not shown), which makes it difficult to accurately quantify its expression above background. Therefore, to pinpoint which CB<sub>1</sub>R-positive interneurons in the HPC contain D<sub>1</sub>R, we combined fluorescence *in situ* hybridization for CB<sub>1</sub>R mRNA in D<sub>1</sub>-Cre and D<sub>1</sub>-CB<sub>1</sub>-KO mice carrying viral Cre-dependent expression of mCherry (STAR Methods; Figure 3B). As described (Marsicano and Lutz, 1999), detectable levels of CB<sub>1</sub>R mRNA were present throughout the HPC in pyramidal neurons and in GABAergic interneurons (Figure S2D). The distribution of mCherry-tagged D<sub>1</sub>-positive neurons in the dorsal CA1 region of D<sub>1</sub>-Cre mice was similar to previous findings (Puighermanal et al., 2017; Gangarossa et al., 2012). Double staining revealed that virtually no high CB<sub>1</sub>R-expressing interneurons in the *strata oriens*, *pyramidale*, *radiatum*, or *lacunosum*

*moleculare* contain D<sub>1</sub>Rs (Figures 3C–3F and S2D). Conversely, D<sub>1</sub>Rs are present in a small subpopulation of low CB<sub>1</sub>R-expressing interneurons along the different hippocampal layers (Figures 3C and 3F). Importantly, this co-expression was virtually abolished in hippocampi of D<sub>1</sub>-CB<sub>1</sub>-KO mice (Figures 3C, 3D, and 3F).

Altogether, these data indicate that CB<sub>1</sub>R-dependent modulation of a small subpopulation of D<sub>1</sub>R-positive GABAergic interneurons is required during NOR memory consolidation.

### Synaptic Mechanisms Underlying NOR Memory Consolidation and Associated Hippocampal Plasticity

The data collected so far show that reduction of GABAergic signaling prevents the deficits in D<sub>1</sub>-CB<sub>1</sub>-KO mice of NOR consolidation. Therefore, we tested whether inhibition of GABA<sub>A</sub> receptors could rescue the lack of learning-induced LTP enhancement observed in D<sub>1</sub>-CB<sub>1</sub>-KO mice. Trained mice received bicuculline or vehicle (VEH) before testing LTP induction in hippocampal circuits. In vehicle-treated animals, D<sub>1</sub>-CB<sub>1</sub>-KO mice showed no training-induced LTP enhancement (Figures 4A–4C). Strikingly, although bicuculline did not affect LTP in WT animals, it rescued the training-induced LTP of D<sub>1</sub>-CB<sub>1</sub>-KO mice (Figures 4A–4C).

Recent data suggest that hippocampal D<sub>1</sub>R-like receptors participate in memory formation, but little is known concerning the cell types involved (Lisman et al., 2011; Yamasaki and Takeuchi, 2017). Our data indicate that CB<sub>1</sub>R-dependent control of GABAergic transmission from a low number of hippocampal interneurons expressing D<sub>1</sub>R is required to guarantee late consolidation of NOR memory. Therefore, it is possible that endocannabinoid actions are secondary to activation of D<sub>1</sub>Rs in these cells. To address this issue, we first reasoned that partial inhibition of D<sub>1</sub>Rs should “replace” the lack of CB<sub>1</sub>R-dependent control of neurotransmission in D<sub>1</sub>-CB<sub>1</sub>-KO mice. Thus, we administered a sub-effective dose of the D<sub>1/5</sub>R antagonist SCH-23390 (Figures S3A–S3C) to D<sub>1</sub>-CB<sub>1</sub>-KO mice and WT littermates after NOR acquisition and analyzed the training-induced enhancement of *in vivo* LTP. This treatment slightly reduced the late phase of LTP in WT animals (Figures 4A–4C). However, the antagonist abolished the differences between D<sub>1</sub>-CB<sub>1</sub>-KO mice and WT littermates (Figures 4A–4C), indicating that reducing D<sub>1</sub>R activity counteracts the absence of CB<sub>1</sub>Rs in the mutants. If LTP is mechanistically linked to NOR consolidation, then the same treatment should rescue the memory impairment of

#### Figure 2. Learning-Induced Facilitation of *In Vivo* Hippocampal LTP Requires CB<sub>1</sub>Rs at D<sub>1</sub>R-Positive Neurons

(A and B) HFS in the dorsal hippocampal CA3 Schaffer collateral pathway induces *in vivo* LTP in the dorsal CA1 *stratum radiatum*.

(A) Summary plots of recorded evoked fEPSPs in anesthetized D<sub>1</sub>-CB<sub>1</sub>-WT (n = 8) and D<sub>1</sub>-CB<sub>1</sub>-KO (n = 8) mice.

(B) Bar histograms of normalized fEPSPs from (A), representing 30 and 60 min after HFS.

(C) Schematic representation of the experimental setup (STAR Methods).

(D and E) Learning modulates *in vivo* LTP.

(D) Summary plots of recorded evoked fEPSPs from mice exposed to control (n = 8) and NOR training (n = 11) conditions.

(E) Bar histograms of normalized evoked fEPSPs from (D), representing 30 and 60 min after HFS.

(F and G) Learning-induced modulation of *in vivo* LTP is impaired in D<sub>1</sub>-CB<sub>1</sub>-KO mice.

(F) Summary plots of recorded fEPSPs in anesthetized D<sub>1</sub>-CB<sub>1</sub>-WT (n = 10) and D<sub>1</sub>-CB<sub>1</sub>-KO (n = 10) mice.

(G) Bar histograms of normalized evoked fEPSPs from (F), representing 30 and 60 min after HFS.

Traces on the right side of the summary plots represent 150 superimposed evoked fEPSPs before HFS (1, gray) and 30 min (2, brown) and 60 min (3, black) after HFS. Data, mean ± SEM. \*p < 0.05. See also Table S1.

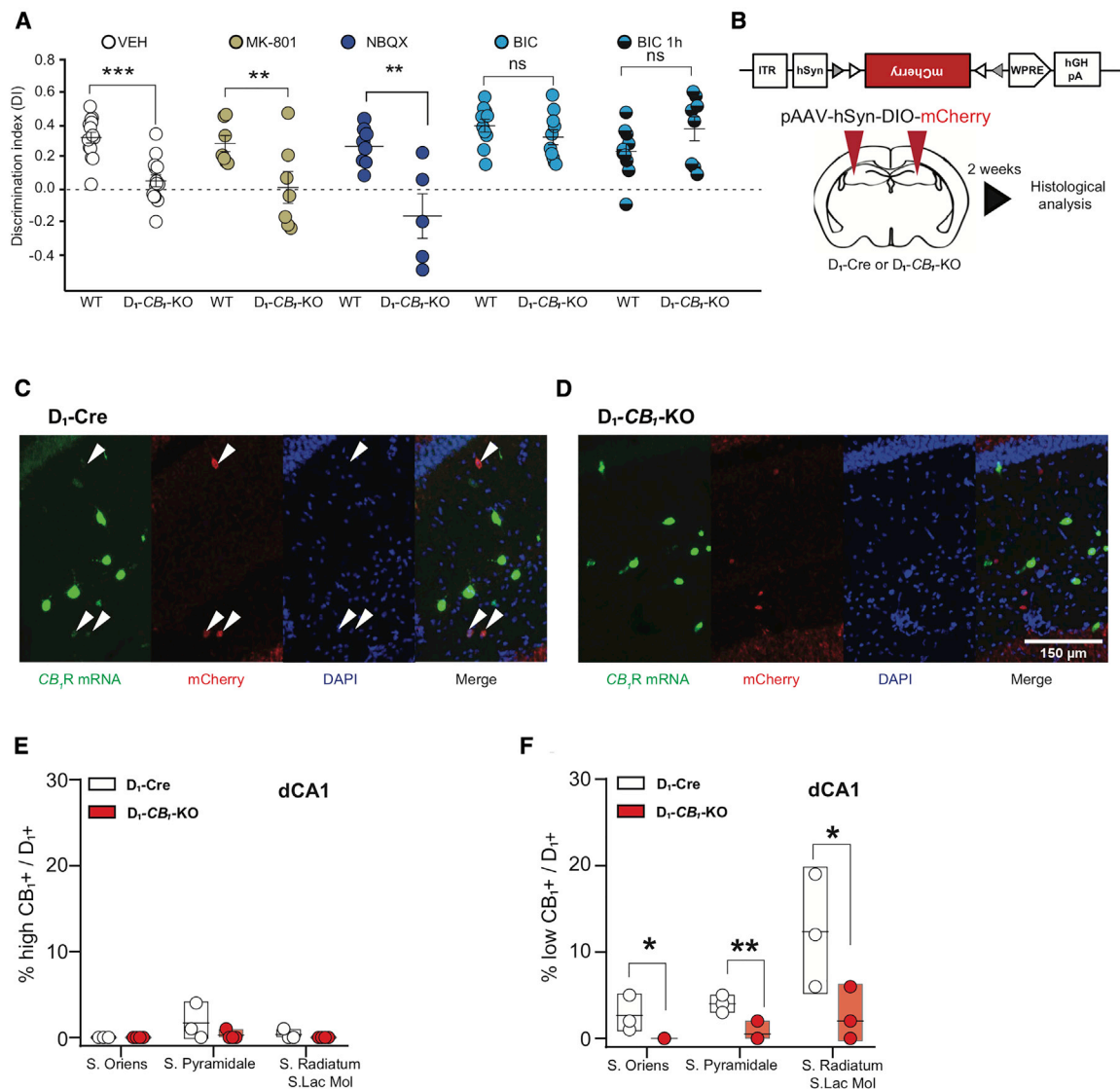


**Figure 3. Hippocampal CB<sub>1</sub>R/D<sub>1</sub>R-Positive Interneurons Modulate Synaptic GABAergic Transmission**

(A) NOR memory performance of mutant mice administered vehicle (n D<sub>1</sub>-CB<sub>1</sub>-WT = 14, n D<sub>1</sub>-CB<sub>1</sub>-KO = 14), MK-801 (0.1 mg/kg, intraperitoneally [i.p.]; n D<sub>1</sub>-CB<sub>1</sub>-WT = 7, n D<sub>1</sub>-CB<sub>1</sub>-KO = 7), NBQX (5 mg/kg, i.p.; n D<sub>1</sub>-CB<sub>1</sub>-WT = 8, n D<sub>1</sub>-CB<sub>1</sub>-KO = 5), or bicuculline immediately after (n D<sub>1</sub>-CB<sub>1</sub>-WT = 10, n D<sub>1</sub>-CB<sub>1</sub>-KO = 10) or 1 h after the training phase (n D<sub>1</sub>-CB<sub>1</sub>-WT = 10, n D<sub>1</sub>-CB<sub>1</sub>-KO = 8).

(B) Schematic representation of the experimental procedure to detect CB<sub>1</sub>R mRNA in D<sub>1</sub>R-positive cells.

(C and D) Representative images of CB<sub>1</sub>R mRNA (green) and mCherry protein (red) labeling in the hippocampal CA1 region of D<sub>1</sub>-Cre (C) and D<sub>1</sub>-CB<sub>1</sub>-KO (D) mice. White arrows indicate colocalization of CB<sub>1</sub>R-positive and D<sub>1</sub>R-positive cell bodies. Scale bar, 150 μm.

(E and F) Layer-specific distribution of the percentage of cell bodies expressing high (E) and low amounts (F) of CB<sub>1</sub>Rs, which colocalize with mCherry-positive (i.e., D<sub>1</sub>R-positive) in D<sub>1</sub>-Cre (n = 3) and D<sub>1</sub>-CB<sub>1</sub>-KO (n = 3).

Data, mean ± SEM. \*p < 0.05, \*\*p < 0.01. See also Figure S2 and Table S1.

D<sub>1</sub>-CB<sub>1</sub>-KO mice. Administration of SCH-23390 did not alter the behavior of WT mice (Figures 4D, S3D, and S3E), but, strikingly, it fully rescued the memory impairment of D<sub>1</sub>-CB<sub>1</sub>-KO littermates (Figures 4D, S3D, and S3E).

Altogether, these results indicate that endocannabinoid-dependent regulation of hippocampal D<sub>1</sub>R-positive interneurons is a necessary step in dopaminergic control of NOR memory consolidation and associated synaptic plasticity.

## DISCUSSION

The present study reveals that a specific subpopulation of hippocampal D<sub>1</sub>R/CB<sub>1</sub>R-positive neurons controls late consolidation of NOR memory and associated synaptic plasticity by moderating local inhibitory GABAergic activity in the HPC. Specifically, CB<sub>1</sub>Rs expressed in D<sub>1</sub>R-positive interneurons participate in learning-induced facilitation of *in vivo* LTP and are required for

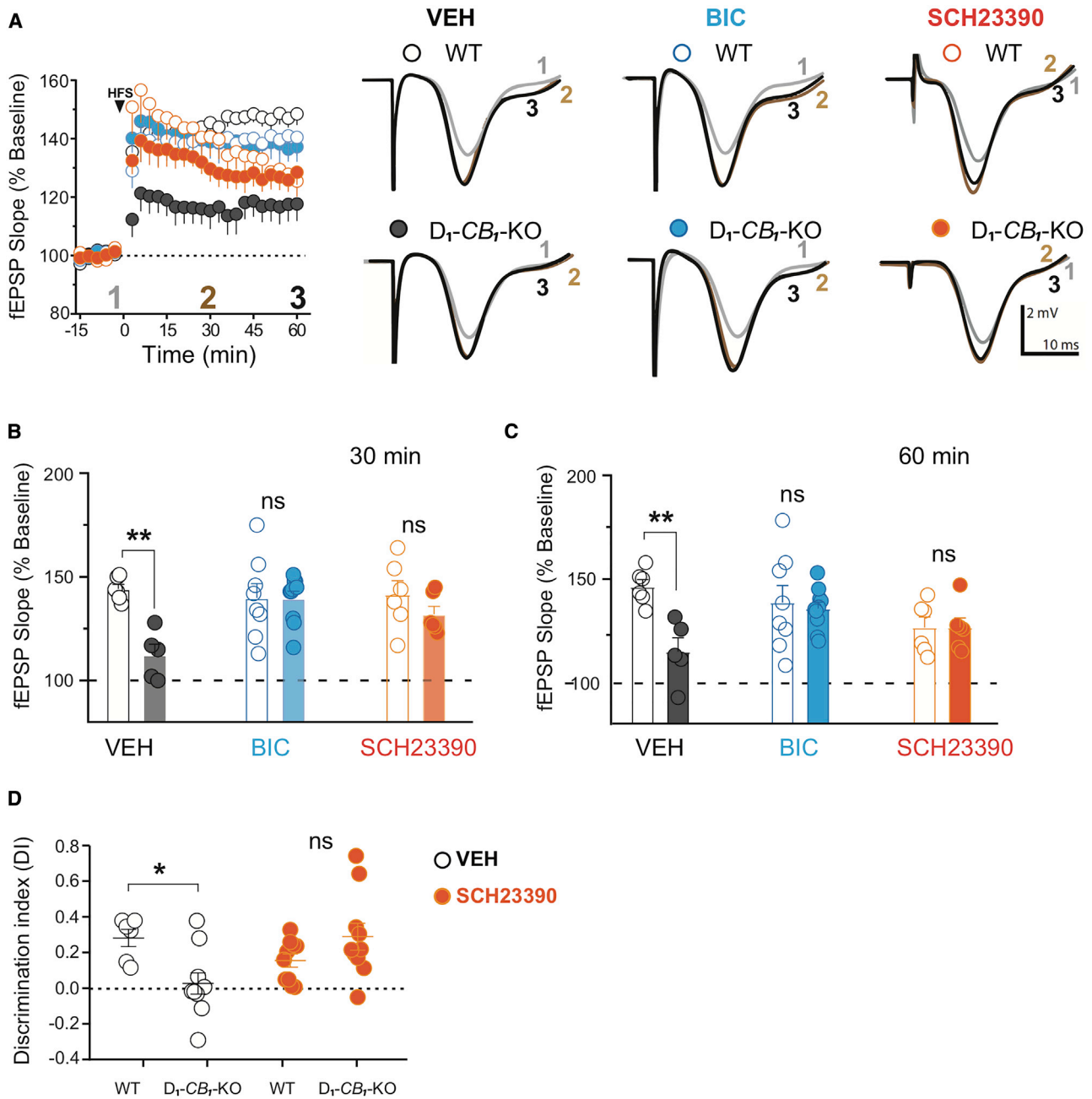


**Figure 4. Cellular Mechanisms Linking D<sub>1</sub>R Signaling with GABAergic Activity during Learning-Induced Facilitation of *In Vivo* LTP and Memory Consolidation**

(A) Effects of the GABA<sub>A</sub> receptor antagonist bicuculline and the D<sub>1/5</sub>R antagonist SCH-23390 on learning-induced modulation of *in vivo* LTP in D<sub>1</sub>-CB<sub>1</sub>-WT and D<sub>1</sub>-CB<sub>1</sub>-KO mice. Shown are summary plots of recorded evoked fEPSPs in vehicle (n D<sub>1</sub>-CB<sub>1</sub>-WT = 6, n D<sub>1</sub>-CB<sub>1</sub>-KO = 8), bicuculline (0.5 mg/kg, i.p.; n D<sub>1</sub>-CB<sub>1</sub>-WT = 9, n D<sub>1</sub>-CB<sub>1</sub>-KO = 11), and SCH-23390 (0.3 mg/kg, i.p.; n D<sub>1</sub>-CB<sub>1</sub>-WT = 6, n D<sub>1</sub>-CB<sub>1</sub>-KO = 6).

(B and C) Bar histograms of (A), representing normalized fEPSPs from 30 (B) and 60 (C) min after HFS.

(D) Memory performance D<sub>1</sub>-CB<sub>1</sub>-WT and D<sub>1</sub>-CB<sub>1</sub>-KO mice after being injected with vehicle (n D<sub>1</sub>-CB<sub>1</sub>-WT = 6, n D<sub>1</sub>-CB<sub>1</sub>-KO = 10) or SCH-23390 (0.3 mg/kg, i.p.; n D<sub>1</sub>-CB<sub>1</sub>-WT = 10, n D<sub>1</sub>-CB<sub>1</sub>-KO = 10).

Traces on the right side of the summary plot (A) represent 150 superimposed evoked fEPSPs before HFS (1, gray) and 30 min (2, brown) and 60 min (3, black) after HFS. Data, mean ± SEM. \*p < 0.05, \*\*p < 0.01.

See also Figure S3 and Table S1.



consolidation of NOR memory. Moreover, CB<sub>1</sub>R<sub>s</sub> in D<sub>1</sub>R-positive neurons are necessary for physiological D<sub>1</sub>R-dependent modulation of memory processes, suggesting that cannabinoid signaling is part of a complex modulatory circuit regulated by dopamine transmission in the HPC. By determining cellular and behavioral functions of a specific CB<sub>1</sub>R-expressing interneuron subpopulation, these data uncover an unforeseen role of CB<sub>1</sub>R<sub>s</sub> in the D<sub>1</sub>R-dependent control of long-term memory.

The endocannabinoid system regulates episodic-like recognition memory processes via CB<sub>1</sub>R-dependent control of different cell types in the HPC (Busquets-Garcia et al., 2017; Soria-Gomez et al., 2017; Busquets Garcia et al., 2016; Puighermanal et al., 2009; Robin et al., 2018). In the present study, we observed that the transition from short- to long-term memory processes is controlled by a functional interaction between D<sub>1</sub>R<sub>s</sub> and CB<sub>1</sub>R<sub>s</sub> in a specific subpopulation of hippocampal interneurons. In contrast, CB<sub>1</sub>R deletion from all body cells or in all forebrain GABAergic neurons does not reproduce the phenotype of D<sub>1</sub>-CB<sub>1</sub>-KO mice (Puighermanal et al., 2009; Hebert-Chatelain et al., 2016). These apparently contrasting observations can be explained by different possibilities. Long-term deletion of the CB<sub>1</sub>R gene starting from early developmental stages in CB<sub>1</sub>-KO and GABA-CB<sub>1</sub>-KO mice might induce compensatory mechanisms (El-Brolosy et al., 2019; El-Brolosy and Stainier, 2017), masking the functional role of the CB<sub>1</sub>R in NOR memory. An alternative or complementary explanation might point to the presence of different subpopulations of brain cells expressing CB<sub>1</sub>R<sub>s</sub> and exerting opposite effects on memory processes. For instance, endocannabinoid signaling might promote or inhibit memory formation when acting at D<sub>1</sub>R-positive cells or at other neuronal subpopulations, respectively. We have shown previously that astroglial CB<sub>1</sub>R<sub>s</sub> are necessary for consolidation of NOR memory by allowing D-serine availability at glutamatergic synapses (Robin et al., 2018). We cannot fully exclude that deletion of CB<sub>1</sub>R<sub>s</sub> in D<sub>1</sub>R-positive cells does not also involve astrocytes (Nagatomo et al., 2017). However, so far, no conclusive anatomical evidence has been presented for expression of D<sub>1</sub>R<sub>s</sub> in hippocampal astrocytes (Chai et al., 2017; Zhang et al., 2014; but see Jennings et al., 2017 for D<sub>1/5</sub>R pharmacological experiments). Moreover, our current and past results suggest that endocannabinoid control of astrocytes is likely involved in the initial phases of memory formation, whereas CB<sub>1</sub>R-dependent inhibition of D<sub>1</sub>R-positive hippocampal interneurons determines later phases of NOR memory consolidation. The time-course effects of pharmacological treatments indicate that D-serine can rescue memory performance of GFAP-CB<sub>1</sub>-KO mice only when administered immediately after learning (Robin et al., 2018). This idea is reinforced by the fact that these mutants do not express *in vivo* LTP even under basal “home cage” conditions (Robin et al., 2018), whereas D<sub>1</sub>-CB<sub>1</sub>-KO mice only lack the specific facilitation of LTP induced by learning. Altogether, these observations allow speculation that at least two distinct temporal windows exist in CB<sub>1</sub>R-dependent control of NOR. First, astroglial CB<sub>1</sub>R are necessary for the plastic processes to initiate the memory. Later, endocannabinoid-dependent regulation of D<sub>1</sub>R-positive interneurons is required to maintain the memory trace for longer periods.

Hippocampal D<sub>1</sub>R have been shown previously to be mainly on GABAergic interneurons, but lower levels were also detected on glutamatergic neurons (Gangarossa et al., 2012; Puighermanal et al., 2017; [http://celltypes.brain-map.org/maseq/mouse\\_ctx-hip\\_smart-seq](http://celltypes.brain-map.org/maseq/mouse_ctx-hip_smart-seq)). Our data show that the D<sub>1</sub>-Cre mouse line used in the present study (Lemberger et al., 2007) induces recombination in a small sub-fraction of hippocampal interneurons containing low levels of CB<sub>1</sub>R mRNA but also in pyramidal neurons and mossy cells. Therefore, we cannot fully exclude that cell types other than hippocampal interneurons might participate in D<sub>1</sub>R/CB<sub>1</sub>R-dependent control of memory consolidation. However, our data show that partial blockade of GABA<sub>A</sub> receptors, but not of AMPA/kainate or NMDA glutamatergic ones, reverse the memory impairment of D<sub>1</sub>-CB<sub>1</sub>-KO mice. Therefore, our findings strongly suggest that CB<sub>1</sub>R control of GABA release from D<sub>1</sub>R-positive interneurons regulates late consolidation of NOR memory. However, recent data using emerging technologies suggest that hippocampal cells are more diverse and functionally segregated than previously thought (Harris et al., 2018; Soltesz and Losonczy, 2018). By identifying specific markers, future studies will extend our genetic and pharmacological evidence that a specific subpopulation of D<sub>1</sub>R/CB<sub>1</sub>R-positive hippocampal interneurons regulates consolidation of NOR memory.

LTP at the CA3-CA1 pathway is a potential molecular and cellular mechanism underlying behavioral expression of episodic-like memory processes (Morris, 2013). Interestingly, although deletion of CB<sub>1</sub>R<sub>s</sub> from D<sub>1</sub>R-positive cells impairs NOR memory, the same manipulation does not impair *in vivo* LTP of hippocampal synaptic transmission in naive animals. In agreement with previous evidence under other experimental conditions (Li et al., 2003; Lemon and Manahan-Vaughan, 2006), WT mice exposed to the NOR learning task display facilitation of *in vivo* LTP compared with animals exposed to the same environment without any learning. Importantly, this facilitation is absent in D<sub>1</sub>-CB<sub>1</sub>-KO mice, suggesting that endocannabinoid control of D<sub>1</sub>R-positive hippocampal interneurons is recruited only after learning. The facilitation might be due to “real” stronger synaptic transmission after learning or a decrease in baseline synaptic activity (Lisman, 2017), which might be occluded in D<sub>1</sub>-CB<sub>1</sub>-KO mice. The fact that partial blockade of GABA<sub>A</sub> receptors in trained WT mice does not alter LTP facilitation suggests that this phenomenon is due to a genuine increase in LTP. In addition, our data indicate that reducing GABAergic transmission in D<sub>1</sub>R-positive neurons is required for this form of learning-induced synaptic plasticity. These results reinforce the idea that, to reveal relevant mechanisms, investigations of synaptic plasticity associated with memory processes should include not only naive animals but also behaviorally challenged ones (Lisman et al., 2011).

D<sub>1</sub>R activity in the HPC is necessary for long-term memory, synaptic plasticity, and network dynamics (Lisman et al., 2011; Yamasaki and Takeuchi, 2017; Kaufman et al., 2020; Bethus et al., 2010). Consistently, our results show that high doses of the D<sub>1/5</sub>R antagonist SCH-23390 impair memory performance in the NOR task. In addition, our data suggest that D<sub>1</sub>R/CB<sub>1</sub>R-positive hippocampal interneurons are one of the targets of dopaminergic control of learning and memory processes. Interestingly, it

has been shown that parvalbumin (PV)-expressing interneurons require D<sub>1</sub>R activity for late phases of memory consolidation through coordinated control of the activity of hippocampal pyramidal neurons (Karunakaran et al., 2016). Particularly, the authors describe that this D<sub>1</sub>R activity modulates hippocampal network oscillations (i.e., sharp-wave ripples), which is a proposed correlate for synaptic plasticity and memory consolidation (Buzsáki, 2015). In addition, previous studies have shown that PV/CB<sub>1</sub>R-negative and CCK/CB<sub>1</sub>R-positive interneurons have complementary roles in ensuring such high oscillatory ripple events with consequent capacity to modulate synaptic plasticity (Klausberger et al., 2005; Buzsáki, 2015). Therefore, we speculate that the subpopulation of D<sub>1</sub>R/CB<sub>1</sub>R-positive interneurons described in our work could play a complementary role in maintaining a proper excitation/inhibition balance in the hippocampal network activity required for memory consolidation.

Although complete elucidation of the complex microcircuitry requires further characterization, our findings support the hypothesis that D<sub>1</sub>R/CB<sub>1</sub>R-positive hippocampal interneurons belong to a broader circuit participating in dopaminergic control of memory (Yamasaki and Takeuchi, 2017). Our data are compatible with a scenario where D<sub>1</sub>R activation during the learning/consolidation process potentiates GABAergic transmission. However, this D<sub>1</sub>R-dependent increase in inhibition is kept within adequate limits by activation of CB<sub>1</sub>Rs, allowing proper flow of information. In this sense, in the absence of CB<sub>1</sub>R-dependent control of D<sub>1</sub>R/CB<sub>1</sub>R-positive interneurons (i.e., D<sub>1</sub>-CB<sub>1</sub>-KO mice), partial inhibition of D<sub>1</sub>-like or GABA<sub>A</sub> receptors rescues the phenotype. In other words, although activation of D<sub>1</sub>Rs in interneurons seems to be necessary for the memory process, their abnormally high activity (e.g. in the absence of CB<sub>1</sub>Rs) impairs such functions. In this context, an interesting question relates to the functional link between endogenous activation of D<sub>1</sub>Rs and CB<sub>1</sub>Rs. Our results allow speculation about two potential scenarios based on autocrine or paracrine modes of action of endocannabinoid signaling (Busquets-García et al., 2017). (1) General D<sub>1</sub>R-dependent dopaminergic signaling in the HPC might activate pyramidal neurons (Roggenhofer et al., 2013; Shivarama Shetty et al., 2016) targeted by D<sub>1</sub>R/CB<sub>1</sub>R-positive interneurons. This depolarization of pyramidal neurons would, in turn, induce canonical endocannabinoid-dependent retrograde inhibition of GABAergic release (Castillo et al., 2012), moderating, among others, activation of D<sub>1</sub>R/CB<sub>1</sub>R-positive interneurons. (2) Following D<sub>1</sub>R activation and consequent interneuron depolarization (Anastasiades et al., 2019; Gorelova et al., 2002), endocannabinoids might be mobilized locally and act in an autocrine manner to decrease the membrane potential and thereby moderate the activity of the neuron (Bacci et al., 2004). These two possibilities are not mutually exclusive, and they might reflect the effect of the mechanisms described on general network activity and/or on specific plastic cellular processes, respectively. Future studies will investigate these intriguing scenarios using adapted experimental approaches.

Altogether, these data reveal that functionally distinct cell types are present in the general population of hippocampal GABAergic interneurons expressing CB<sub>1</sub>Rs. In particular, D<sub>1</sub>R/CB<sub>1</sub>R-positive interneurons provide specific behavioral and hippocampal synaptic mechanisms sustaining the fine-tuned regulation of memory

processes. The close interaction of CB<sub>1</sub>Rs and D<sub>1</sub>Rs in modulating recognition memory might provide novel therapeutic frameworks for treatment of cognitive diseases characterized by alterations of endocannabinoid or dopaminergic systems or both.

## STAR★METHODS

Detailed methods are provided in the online version of this paper and include the following:

- KEY RESOURCES TABLE
- RESOURCE AVAILABILITY
  - Lead Contact
  - Materials Availability
  - Data and Code Availability
- EXPERIMENTAL MODEL AND SUBJECT DETAILS
  - Animal Model
- METHOD DETAILS
  - Drug preparation and administration
  - Novel object recognition memory
  - *In vivo* electrophysiology in anesthetized mice
  - Surgery and viral administration
  - Immunohistochemistry on free-floating sections
  - Combined Fluorescent *in situ* hybridization (FISH)/Immunohistochemistry (IHC) on free-floating frozen sections
- QUANTIFICATION AND STATISTICAL ANALYSIS
  - Data collection
  - Fluorescence quantifications
  - Statistical analyses

## SUPPLEMENTAL INFORMATION

Supplemental Information can be found online at <https://doi.org/10.1016/j.celrep.2020.108046>.

## ACKNOWLEDGMENTS

We thank Delphine Gonzales, Nathalie Aubailly, and the personnel of the Animal Facilities of the NeuroCentre Magendie for mouse care. We thank the Biochemistry Platform of Bordeaux NeuroCampus and the members of Marsicano's lab for useful discussions. This work was funded by INSERM; the European Research Council (Endofood ERC-2010-StG-260515, CannaPreg ERC-2014-PoC-640923, and MiCaBra ERC-2017-AdG-786467 to G.M.); Fondation pour la Recherche Médicale (FRM; DRM20101220445 to G.M. and DT20160435664 to J.F.O.d.C.); the Human Frontiers Science Program, Region Aquitaine, Agence Nationale de la Recherche (ANR; NeuroNutriSens ANR-13-BSV4-0006, ORUPS ANR-16-CE37-0010-01, and CaCoVi ANR-18-CE16-0001-02 to G.M.); BRAIN ANR-10-LABX-0043 (to G.M.); NIH/NIDA (1R21DA037678-01); the European Regional Development Fund; the European Union Horizon 2020 Research and Innovation Program (grant agreement 686009); French State/Agence Nationale de la Recherche/IdEx (ANR-10-IDEX-03-02), Eu-Fp7 (FP7-PEOPLE-2013-IEF-623638), and MINECO/AEI (RYC-2017-21776) (to A.B.-G.); FRM (ARF20140129235 to L.B.); and Ikerbasque (The Basque Foundation for Science) and MINECO (Ministerio de Economía y Competitividad) PGC2018-093990-A-I00 (MICIU/AEI/FEDER, UE) (to E.S.-G.).

## AUTHOR CONTRIBUTIONS

J.F.O.d.C., A.B.-G., G.M., and E.S.-G. conceived and supervised the whole project. J.F.O.d.C. performed and analyzed *in vivo* electrophysiology and

behavioral experiments. A.B.-G. and E.S.-G. performed and analyzed behavioral experiments. L.B. and A.C. contributed to experiments using viral vectors. L.R. and G.L. contributed to behavioral experiments. M.V., F.J.-K., T.L.-L., and M.M. performed cytochemical experiments. Z.Z. and M.V. helped with analysis of the data. J.F.O.d.C., A.B.-G., G.M., and E.S.-G. wrote the manuscript. F.D. contributed to writing. All authors edited and approved the manuscript.

#### DECLARATION OF INTERESTS

The authors declare no competing interests.

Received: October 31, 2019

Revised: June 15, 2020

Accepted: July 27, 2020

Published: August 18, 2020

#### REFERENCES

- Aggleton, J.P., and Morris, R.G.M. (2018). Memory: Looking back and looking forward. *Brain Neurosci. Adv.* 2, 2398212818794830.
- Anastasiades, P.G., Boada, C., and Carter, A.G. (2019). Cell-Type-Specific D1 Dopamine Receptor Modulation of Projection Neurons and Interneurons in the Prefrontal Cortex. *Cereb. Cortex* 29, 3224–3242.
- Atasoy, D., Aponte, Y., Su, H.H., and Sternson, S.M. (2008). A FLEX switch targets Channelrhodopsin-2 to multiple cell types for imaging and long-range circuit mapping. *J. Neurosci.* 28, 7025–7030.
- Bacci, A., Huguenard, J.R., and Prince, D.A. (2004). Long-lasting self-inhibition of neocortical interneurons mediated by endocannabinoids. *Nature* 431, 312–316.
- Bethus, I., Tse, D., and Morris, R.G. (2010). Dopamine and memory: modulation of the persistence of memory for novel hippocampal NMDA receptor-dependent paired associates. *J. Neurosci.* 30, 1610–1618.
- Busquets-García, A., Puighearnal, E., Pastor, A., de la Torre, R., Maldonado, R., and Ozaita, A. (2011). Differential role of anandamide and 2-arachidonoylglycerol in memory and anxiety-like responses. *Biol. Psychiatry* 70, 479–486.
- Busquets-García, A., Gomis-González, M., Guegan, T., Agustín-Pavón, C., Pastor, A., Mato, S., Pérez-Samartín, A., Matute, C., de la Torre, R., Dierssen, M., et al. (2013). Targeting the endocannabinoid system in the treatment of fragile X syndrome. *Nat. Med.* 19, 603–607.
- Busquets-García, A., Desprez, T., Metna-Laurent, M., Bellocchio, L., Marsicano, G., and Soria-Gomez, E. (2015). Dissecting the cannabinergic control of behavior: The where matters. *BioEssays* 37, 1215–1225.
- Busquets Garcia, A., Soria-Gomez, E., Bellocchio, L., and Marsicano, G. (2016). Cannabinoid receptor type-1: breaking the dogmas. *F1000Res.* 5, 5.
- Busquets-García, A., Bains, J., and Marsicano, G. (2017). CB1 Receptors Signaling in the Brain: Extracting Specificity from Ubiquity. *Neuropsychopharmacology* 43, 4–20.
- Buzsáki, G. (2015). Hippocampal sharp wave-ripple: A cognitive biomarker for episodic memory and planning. *Hippocampus* 25, 1073–1188.
- Castillo, P.E., Younts, T.J., Chávez, A.E., and Hashimoto, Y. (2012). Endocannabinoid signaling and synaptic function. *Neuron* 76, 70–81.
- Chai, H., Diaz-Castro, B., Shigetomi, E., Monte, E., Oceau, J.C., Yu, X., Cohn, W., Rajendran, P.S., Vondriska, T.M., Whitelegge, J.P., et al. (2017). Neural Circuit-Specialized Astrocytes: Transcriptomic, Proteomic, Morphological, and Functional Evidence. *Neuron* 95, 531–549.e9.
- Darvas, M., and Palmiter, R.D. (2009). Restriction of dopamine signaling to the dorsolateral striatum is sufficient for many cognitive behaviors. *Proc. Natl. Acad. Sci. USA* 106, 14664–14669.
- El-Brolosy, M.A., and Stainier, D.Y.R. (2017). Genetic compensation: A phenomenon in search of mechanisms. *PLoS Genet.* 13, e1006780.
- El-Brolosy, M.A., Kontarakis, Z., Rossi, A., Kuenne, C., Günther, S., Fukuda, N., Kikhi, K., Boezio, G.L.M., Takacs, C.M., Lai, S.L., et al. (2019). Genetic compensation triggered by mutant mRNA degradation. *Nature* 568, 193–197.
- Frey, U., Schroeder, H., and Matthies, H. (1990). Dopaminergic antagonists prevent long-term maintenance of posttetanic LTP in the CA1 region of rat hippocampal slices. *Brain Res.* 522, 69–75.
- Gangarossa, G., Longueville, S., De Bundel, D., Perroy, J., Hervé, D., Girault, J.A., and Valjent, E. (2012). Characterization of dopamine D1 and D2 receptor-expressing neurons in the mouse hippocampus. *Hippocampus* 22, 2199–2207.
- Gomez, J.L., Bonaventura, J., Lesniak, W., Mathews, W.B., Syya-Shah, P., Rodriguez, L.A., Ellis, R.J., Richie, C.T., Harvey, B.K., Dannals, R.F., et al. (2017). Chemogenetics revealed: DREADD occupancy and activation via converted clozapine. *Science* 357, 503–507.
- Gorelova, N., Seamans, J.K., and Yang, C.R. (2002). Mechanisms of dopamine activation of fast-spiking interneurons that exert inhibition in rat prefrontal cortex. *J. Neurophysiol.* 88, 3150–3166.
- Granado, N., Ortiz, O., Suárez, L.M., Martín, E.D., Ceña, V., Solís, J.M., and Moratalla, R. (2008). D1 but not D5 dopamine receptors are critical for LTP, spatial learning, and LTP-Induced arc and zif268 expression in the hippocampus. *Cereb. Cortex* 18, 1–12.
- Harris, K.D., Hochgerner, H., Skene, N.G., Magno, L., Katona, L., Bengtsson Gonzales, C., Somogyi, P., Kessaris, N., Linnarsson, S., and Hjerling-Leffler, J. (2018). Classes and continua of hippocampal CA1 inhibitory neurons revealed by single-cell transcriptomics. *PLoS Biol.* 16, e2006387.
- Hebert-Chatelain, E., Desprez, T., Serrat, R., Bellocchio, L., Soria-Gomez, E., Busquets-García, A., Pagano Zottola, A.C., Delamarre, A., Cannich, A., Vincent, P., et al. (2016). A cannabinoid link between mitochondria and memory. *Nature* 539, 555–559.
- Jennings, A., Tyurikova, O., Bard, L., Zheng, K., Semyanov, A., Henneberger, C., and Rusakov, D.A. (2017). Dopamine elevates and lowers astroglial Ca<sup>2+</sup> through distinct pathways depending on local synaptic circuitry. *Glia* 65, 447–459.
- Karunakaran, S., Chowdhury, A., Donato, F., Quairiaux, C., Michel, C.M., and Caroni, P. (2016). PV plasticity sustained through D1/5 dopamine signaling required for long-term memory consolidation. *Nat. Neurosci.* 19, 454–464.
- Katona, I., and Freund, T.F. (2012). Multiple functions of endocannabinoid signaling in the brain. *Annu. Rev. Neurosci.* 35, 529–558.
- Katona, I., Sperlág, B., Sík, A., Káfalvi, A., Vizi, E.S., Mackie, K., and Freund, T.F. (1999). Presynaptically located CB1 cannabinoid receptors regulate GABA release from axon terminals of specific hippocampal interneurons. *J. Neurosci.* 19, 4544–4558.
- Kaufman, A.M., Geiller, T., and Losonczy, A. (2020). A Role for the Locus Coeruleus in Hippocampal CA1 Place Cell Reorganization during Spatial Reward Learning. *Neuron* 105, 1018–1026.e4.
- Klausberger, T., and Somogyi, P. (2008). Neuronal diversity and temporal dynamics: the unity of hippocampal circuit operations. *Science* 321, 53–57.
- Klausberger, T., Marton, L.F., O'Neill, J., Huck, J.H., Dalezios, Y., Fuentealba, P., Suen, W.Y., Papp, E., Kaneko, T., Watanabe, M., et al. (2005). Complementary roles of cholecystokinin- and parvalbumin-expressing GABAergic neurons in hippocampal network oscillations. *J. Neurosci.* 25, 9782–9793.
- Lemberger, T., Parlato, R., Dassel, D., Westphal, M., Casanova, E., Turiault, M., Tronche, F., Schiffrmann, S.N., and Schütz, G. (2007). Expression of Cre recombinase in dopaminergic neurons. *BMC Neurosci.* 8, 4.
- Lemon, N., and Manahan-Vaughan, D. (2006). Dopamine D1/D5 receptors gate the acquisition of novel information through hippocampal long-term potentiation and long-term depression. *J. Neurosci.* 26, 7723–7729.
- Li, S., Cullen, W.K., Anwyl, R., and Rowan, M.J. (2003). Dopamine-dependent facilitation of LTP induction in hippocampal CA1 by exposure to spatial novelty. *Nat. Neurosci.* 6, 526–531.
- Lisman, J. (2017). Criteria for identifying the molecular basis of the engram (CaMKII, PKMzeta). *Mol. Brain* 10, 55.
- Lisman, J., Grace, A.A., and Duzel, E. (2011). A neoHebbian framework for episodic memory: role of dopamine-dependent late LTP. *Trends Neurosci.* 34, 536–547.

- Marsicano, G., and Kuner, R. (2008). Anatomical distribution of receptors, ligands and enzymes in the brain and the spinal cord: circuitries and neurochemistry. In *Cannabinoids and the brain*, A. Kofalvi, ed. (Springer).
- Marsicano, G., and Lutz, B. (1999). Expression of the cannabinoid receptor CB1 in distinct neuronal subpopulations in the adult mouse forebrain. *Eur. J. Neurosci.* *11*, 4213–4225.
- Marsicano, G., Goodenough, S., Monory, K., Hermann, H., Eder, M., Cannich, A., Azad, S.C., Cascio, M.G., Gutiérrez, S.O., van der Stelt, M., et al. (2003). CB1 cannabinoid receptors and on-demand defense against excitotoxicity. *Science* *302*, 84–88.
- Monory, K., Blaudzun, H., Massa, F., Kaiser, N., Lemberger, T., Schütz, G., Wotjak, C.T., Lutz, B., and Marsicano, G. (2007). Genetic dissection of behavioural and autonomic effects of Delta(9)-tetrahydrocannabinol in mice. *PLoS Biol.* *5*, e269.
- Morris, R.G. (2013). NMDA receptors and memory encoding. *Neuropharmacology* *74*, 32–40.
- Nagatomo, K., Suga, S., Saitoh, M., Kogawa, M., Kobayashi, K., Yamamoto, Y., and Yamada, K. (2017). Dopamine D1 Receptor Immunoreactivity on Fine Processes of GFAP-Positive Astrocytes in the Substantia Nigra Pars Reticulata of Adult Mouse. *Front. Neuroanat.* *11*, 3.
- Nicoll, R.A. (2017). A Brief History of Long-Term Potentiation. *Neuron* *93*, 281–290.
- Oliveira da Cruz, J.F., Robin, L.M., Drago, F., Marsicano, G., and Metna-Laurent, M. (2016). Astroglial type-1 cannabinoid receptor (CB1): A new player in the tripartite synapse. *Neuroscience* *323*, 35–42.
- Parra, P., Gulyás, A.I., and Miles, R. (1998). How many subtypes of inhibitory cells in the hippocampus? *Neuron* *20*, 983–993.
- Pelkey, K.A., Chittajallu, R., Craig, M.T., Tricoire, L., Wester, J.C., and McBain, C.J. (2017). Hippocampal GABAergic Inhibitory Interneurons. *Physiol. Rev.* *97*, 1619–1747.
- Puighermanal, E., Marsicano, G., Busquets-García, A., Lutz, B., Maldonado, R., and Ozaita, A. (2009). Cannabinoid modulation of hippocampal long-term memory is mediated by mTOR signaling. *Nat. Neurosci.* *12*, 1152–1158.
- Puighermanal, E., Busquets-García, A., Gomis-González, M., Marsicano, G., Maldonado, R., and Ozaita, A. (2013). Dissociation of the pharmacological effects of THC by mTOR blockade. *Neuropsychopharmacology* *38*, 1334–1343.
- Puighermanal, E., Cutando, L., Boubaker-Vitre, J., Honoré, E., Longueville, S., Hervé, D., and Valjent, E. (2017). Anatomical and molecular characterization of dopamine D1 receptor-expressing neurons of the mouse CA1 dorsal hippocampus. *Brain Struct. Funct.* *222*, 1897–1911.
- Robin, L.M., Oliveira da Cruz, J.F., Langlais, V.C., Martin-Fernandez, M., Metna-Laurent, M., Busquets-García, A., Bellocchio, L., Soria-Gomez, E., Poupin, T., Varilh, M., et al. (2018). Astroglial CB1 Receptors Determine Synaptic D-Serine Availability to Enable Recognition Memory. *Neuron* *98*, 935–944.e5.
- Robinson, S., and Adelman, J.S. (2015). A Method for Remotely Silencing Neural Activity in Rodents During Discrete Phases of Learning. *J. Vis. Exp.* (100), e52859.
- Roggenhofer, E., Fidzinski, P., Shor, O., and Behr, J. (2013). Reduced threshold for induction of LTP by activation of dopamine D1/D5 receptors at hippocampal CA1-subiculum synapses. *PLoS ONE* *8*, e62520.
- Shivarama Shetty, M., Gopinadhan, S., and Sajikumar, S. (2016). Dopamine D1/D5 receptor signaling regulates synaptic cooperation and competition in hippocampal CA1 pyramidal neurons via sustained ERK1/2 activation. *Hippocampus* *26*, 137–150.
- Sołtesz, I., and Losonczy, A. (2018). CA1 pyramidal cell diversity enabling parallel information processing in the hippocampus. *Nat. Neurosci.* *21*, 484–493.
- Soria-Gomez, E., Metna, M., Bellocchio, L., Busquets-García, A., and Marsicano, G. (2017). The endocannabinoid system in the control of behavior. In *Handbook of Neurobehavioral Genetics and Phenotyping*, V. Tucci, ed. (John Wiley & Sons), pp. 323–355.
- Squire, L.R., Wixted, J.T., and Clark, R.E. (2007). Recognition memory and the medial temporal lobe: a new perspective. *Nat. Rev. Neurosci.* *8*, 872–883.
- Takeuchi, T., Duzkiewicz, A.J., Sonneborn, A., Spooner, P.A., Yamasaki, M., Watanabe, M., Smith, C.C., Fernández, G., Deisseroth, K., Greene, R.W., and Morris, R.G. (2016). Locus coeruleus and dopaminergic consolidation of everyday memory. *Nature* *537*, 357–362.
- Terral, G., Busquets-García, A., Varilh, M., Achicallende, S., Cannich, A., Bellocchio, L., Bonilla-Del Río, I., Massa, F., Puente, N., Soria-Gómez, E., et al. (2019). CB1 receptors in the anterior piriform cortex control odor preference memory. *Curr. Biol.* *29*, 2455–2464.e5.
- Terzian, A.L., Drago, F., Wotjak, C.T., and Micale, V. (2011). The Dopamine and Cannabinoid Interaction in the Modulation of Emotions and Cognition: Assessing the Role of Cannabinoid CB1 Receptor in Neurons Expressing Dopamine D1 Receptors. *Front. Behav. Neurosci.* *5*, 49.
- Whitlock, J.R., Heynen, A.J., Shuler, M.G., and Bear, M.F. (2006). Learning induces long-term potentiation in the hippocampus. *Science* *313*, 1093–1097.
- Yamasaki, M., and Takeuchi, T. (2017). Locus Coeruleus and Dopamine-Dependent Memory Consolidation. *Neural Plast.* *2017*, 8602690.
- Zhang, Y., Chen, K., Sloan, S.A., Bennett, M.L., Scholze, A.R., O’Keefe, S., Phatnani, H.P., Guarnieri, P., Caneda, C., Ruderisch, N., et al. (2014). An RNA-sequencing transcriptome and splicing database of glia, neurons, and vascular cells of the cerebral cortex. *J. Neurosci.* *34*, 11929–11947.

## STAR★METHODS

### KEY RESOURCES TABLE

REAGENT or RESOURCE	SOURCE	IDENTIFIER
<b>Antibodies</b>		
Rabbit antibody against the C-myc epitope tag	BioLegend	Cat# 906301; RRID:AB_2565064
Goat anti-rabbit antibody Alexa Fluor 488	Fisher Scientific	Cat# A-11008; RRID:AB_143165
4',6-diamidino-2-phenylindole	Fisher Scientific	Cat# D3571; RRID:AB_2307445
Rabbit polyclonal antibody against DsRed	Takara Bio	Cat# 632496; RRID:AB_10013483
Secondary antibody goat anti-rabbit conjugated to a horseradish peroxidase	Cell signaling	Cat#7074S; RRID:AB_2099233
Digoxigenin (DIG)-labeled riboprobe against mouse CB <sub>1</sub>	Marsicano and Lutz, 1999	N/A
Anti-DIG antibody conjugated to HRP	Roche	Cat#11207733910; RRID:AB_514500
<b>Bacterial and Virus Strains</b>		
rAAV-CAG-DIO	Lead contact lab	rAAV-30
AAV-CAG-DIO-CB <sub>1</sub>	Lead contact lab	rAAV-37
AAV-CAG-DIO-CB <sub>1</sub> -myc	Lead contact lab	rAAV-21
hSyn-DIO-hM4D(Gi)-mCherry	Addgene	44361-AAV8
pAAV-hSyn-DIO-mCherry	Addgene	50459-AAV8
<b>Chemicals, Peptides, and Recombinant Proteins</b>		
2-methylbutane	Sigma-Aldrich	M32631-1L
TSA plus fluorescein system	Perkin Elmer	NEL741001KT
Streptavidin-Texas Red	Perkin Elmer	NEL721001EA
Normal donkey serum	Merck	S30-100ML
Sheep Serum	Sigma Aldrich	S3772-10ML
Formaldehyde 4%	Sigma Aldrich	HT501128-4L
Blocking reagent (to prepare NEN)	Perkin Elmer	FP1012
TSA Biotin Systems	Perkin Elmer	NEL700A001KT
SSC 20X	Sigma	93017-10L-F
Fluoromount-GSlide Mounting Medium	Electron microscopy sciences	17984-25
Isoflurane	Virbac	Vnr137317
Bicuculine	Sigma-Aldrich	14343-50MG
SCH 23390	Sigma-Aldrich	D054-10MG
MK-801	Sigma-Aldrich	77086-22-7
clozapine-N-oxide CNO	Tocris	4936
<b>Critical Commercial Assays</b>		
Avidin/Biotin Blocking Kit	Vector Labs	SP-2001
<b>Experimental Models: Organisms/Strains</b>		
D <sub>1</sub> -CB <sub>1</sub> -WT and D <sub>1</sub> -CB <sub>1</sub> -KO	Lead contact lab	N/A
C57BL/6N	Janvier Labs	C57BL/6NRj
D <sub>1</sub> -Cre	Lead contact lab	Tg(Drd1a-cre)AGsc/KndIJ,
CB <sub>1</sub> <sup>flax/flax</sup>	Lead contact lab	Cnr1tm1.2Ltz, MGI:3045419
GFAP-CB <sub>1</sub> -WT and GFAP-CB <sub>1</sub> -KO	Lead contact lab	N/A
<b>Software and Algorithms</b>		
Prism	Graphpad Software	V6.0
CED 1401 Spike2	Cambridge Electronic Design	V6.18
ImageJ	NIH	V1.52

## RESOURCE AVAILABILITY

### Lead Contact

Further information and requests for resources and reagents should be directed to and will be fulfilled by the Lead Contact, Giovanni Marsicano ([giovanni.marsicano@inserm.fr](mailto:giovanni.marsicano@inserm.fr)).

### Materials Availability

Mouse lines generated and used in the current study are available from the lead contact upon request. We are glad to share the mouse lines with reasonable compensation by requestor for its processing and shipping.

### Data and Code Availability

The data supporting the current study have not been deposited in a public repository but are available from the lead contact on request.

## EXPERIMENTAL MODEL AND SUBJECT DETAILS

### Animal Model

All experimental procedures were approved by the ethical committee of the French Ministry of Higher Education, Research and Innovation (authorization APAFIS#18111). Maximal efforts were made to reduce the suffering of the animals. Male mice were used in this study.

$D_1$ - $CB_1$ -KO mice were generated as previously described (Monory et al., 2007; Terzian et al., 2011). Briefly,  $CB_1$  floxed mice (Marsicano et al., 2003) were crossed with  $D_1$ -Cre line (Lemberger et al., 2007), in which the Cre recombinase was placed under the control of the  $D_1$  gene (*Drd1a*) regulatory sequences using transgenesis with modified bacterial artificial chromosomes. The pattern of Cre expression recapitulated the expression pattern of the endogenous *Drd1a* (Lemberger et al., 2007). Breeding was performed by mating male Cre-positive  $D_1$ - $CB_1$ -KO mice with homozygous  $CB_1$ -flox female mice deriving from a separate colony. In order to detect possible germline or ectopic recombination events, genotyping of tail samples from pups (PD10) was performed by genomic PCR using primers suited to identify WT, “floxed” and “recombined” bands. No germline or ectopic recombination was detected. Eight to 14 weeks-old naive male  $D_1$ - $CB_1$ -KO and WT littermates were used. 8-14 weeks old male C57BL/6NRj mice purchased from Janvier (France). 8-12 weeks-old  $D_1$ -Cre mice bred in the animal facilities of the U1215 we also used. Animals were housed collectively under standard conditions of temperature and humidity in a day/night cycle of 12/12 hours (light on at 7 am). Animals that underwent surgery were kept in individual cages after the procedures to avoid conflict with their littermates. Food and water were provided *ad libitum*. All the experiments were performed during the light phase. Behavioral experiments were performed from 9 am to 3 pm. Electrophysiology experiments were performed from 8 am to 7 pm.

## METHOD DETAILS

### Drug preparation and administration

Bicuculline, MK-801, NBQX and SCH-23390 were purchased from Merck (formerly Sigma-Aldrich, France) and were dissolved to their final concentration in physiological saline (NaCl 0.9%). The exogenous DREADD ligand clozapine-N-oxide (CNO, 2 mg/kg) was purchased from Tocris Bioscience (Bristol, UK) and dissolved in saline after gently mixing with a vortex. All drugs were injected intraperitoneally in a volume of 10 ml/kg. Vehicle in all the conditions was composed of physiological saline (NaCl 0.9%) injections.

### Novel object recognition memory

We used the novel object recognition (NOR) memory task in an L-maze (Busquets-Garcia et al., 2011, 2013; Hebert-Chatelain et al., 2016; Puighermanal et al., 2009, 2013; Robin et al., 2018).

The task took place in a L-shaped maze made of dark gray polyvinyl chloride made by two identical perpendicular arms (35 cm and 30 cm long respectively for external and internal L walls, 4.5cm wide and 15 cm high walls) placed on a white background (Busquets-Garcia et al., 2011; Puighermanal et al., 2009). The task occurred in a room adjacent to the animal house with a light intensity fixed at 50 lux. The maze was overhung by a video camera allowing the detection and offline scoring of animal's behavior. The task consisted in 3 sequential daily trials of 9 minutes each. During the habituation phase (day 1), mice were placed in the center of the maze and allowed to freely explore the arms in the absence of any objects. The training phase (day 2) consisted in placing the mice again in the corner of the maze in the presence of two identical objects positioned at the extremities of each arm and left to freely explore the maze and the objects. The testing phase occurred 24 hours later (day 3): one of the familiar objects was replaced by a novel object different in its shape, color and texture and mice were left to explore both objects. The position of the novel object and the associations of novel and familiar were randomized. All objects were previously tested to avoid biased preference. Memory performance was assessed by the discrimination index (DI). The DI was calculated as the difference between the time spent exploring the novel (TN) and the familiar object (TF) divided by the total exploration time (TN+TF):  $DI = [TN - TF] / [TN + TF]$ . Memory was also evaluated by directly comparing the exploration time of novel and familiar objects, respectively. Object exploration was defined as the orientation

of the nose to the object at less than 2 cm. Experienced investigators evaluating the exploration were blind of treatment and/or genotype of the animals. Pharmacological treatments were immediately administered after the training phase.

### ***In vivo* electrophysiology in anesthetized mice**

Experiments were performed as described in [Robin et al. \(2018\)](#). Mice were anesthetized in a box containing 5% Isoflurane (Virbac, France) before being placed in a stereotaxic frame (Model 900, Kopf instruments, CA, USA) in which 1.0% to 1.5% of Isoflurane was continuously supplied via an anesthetic mask during the whole duration of the experiment. The body temperature was maintained at  $\pm 36.5^\circ\text{C}$  using a homeothermic system (model 50-7087-F, Harvard Apparatus, MA, USA) and the state of anesthesia was assessed by mild tail pinch. Before surgery, 100 mL of the local anesthetic lurocaine (vetoquinol, France) was injected in the scalp region. Surgical procedure started with a longitudinal incision of 1.5 cm in length aimed to expose Bregma and Lambda. After ensuring the correct alignment of the head, two holes were drilled in the skull for electrode placement. Glass recording electrodes were inserted in the CA1 stratum radiatum, and a concentric stimulating bipolar electrode (Model CBARC50, FHC, ME, USA) placed in the CA3 region. Coordinates were as follows: CA1 stratum radiatum: A/P 1.5, M/L 1.0, DV 1.20; CA3: A/P 2.2, M/L 2.8, D/V 1.3 (20 insertion angle). The recording electrode (tip diameter = 1–2 mm, 2–4 M $\Omega$ ) was filled with a 2% pontamine sky blue solution in 0.5M sodium acetate. At first the recording electrode was placed by hand until it reached the surface of the brain and then to the final depth using a hydraulic micro-positioner (Model 2650, KOPF instruments, CA, USA). The stimulation electrode was placed in the correct area using a standard manipulator. Both electrodes were adjusted to find the area with maximum response. *In vivo* recordings of evoked field excitatory postsynaptic potentials (fEPSPs) were amplified 1000 times and filtered (low-pass at 1Hz and high-pass 3000Hz) by a DAGAN 2400A amplifier (DAGAN Corporation, MN, USA). fEPSPs were digitized and collected on-line using a laboratory interface and software (CED 1401, SPIKE 2; Cambridge Electronic Design, Cambridge, UK). Test pulses were generated through an Isolated Constant Current Stimulator (DS3, Digitimer, Hertfordshire, UK) triggered by the SPIKE 2 output sequencer via CED 1401 and collected every 2 s at a 10 kHz sampling frequency and then averaged every 180 s. Test pulse intensities were typically between 40–250  $\mu\text{A}$  with a duration of 50 ms. Basal stimulation intensity was adjusted to 30%–50% of the current intensity that evoked a maximum field response. All responses were expressed as percent from the average responses recorded during the 15 min before high frequency stimulation (HFS). HFS was induced by applying 3 trains of 100 Hz (1 s each), separated by 20 s interval. fEPSP were then recorded for a period of 60 min. C57BL6/NRj mice underwent this *in vivo* electrophysiology procedure after the training phase of NOR task. Also, where specified, D<sub>1</sub>-CB<sub>1</sub>-KO and D<sub>1</sub>-CB<sub>1</sub>-WT received an injection of Bicuculine (0.5 mg/kg, intraperitoneal) or SCH 23390 (0.3 mg/kg, intraperitoneal) or vehicle immediately after undergoing training in NOR and before being subjected to the *in vivo* electrophysiology procedure. At the end the experiment, the position of the electrodes was marked (recording area: iontophoretic infusion of the recording solution during 180 s at 20mA; stimulation area: continuous current discharge over 20 s at +20mA) and histological verification was performed *ex vivo*.

### **Surgery and viral administration**

Mice were anesthetized in a box containing 5% Isoflurane (Virbac, France) before being placed in a stereotaxic frame (Model 900, Kopf instruments, CA, USA) in which 1.0% to 1.5% of Isoflurane was continuously supplied via an anesthetic mask during the whole duration of the experiment. For viral intra-HPC AAV delivery, mice were submitted to stereotaxic surgery (as above) and AAV vectors were injected with the help of a microsyringe (0.25 mL Hamilton syringe with a 30-gauge beveled needle) attached to a pump (UMP3-1, World Precision Instruments, FL, USA). Where specified, D<sub>1</sub>-CB<sub>1</sub>-WT and D<sub>1</sub>-CB<sub>1</sub>-KO mice were injected directly into the hippocampus (HPC) or striatum (STR) (0.5  $\mu\text{l}$  per injection site at a rate of 0.5  $\mu\text{l}$  per min), with the following coordinates: HPC, AP  $-1.8$ ; ML  $\pm 1$ ; DV  $-2.0$  and  $-1.5$ ; Striatum: AP  $-1.34$ ; ML  $\pm 2.8$ ; DV  $-1.84$ . Following virus delivery, the syringe was left in place for 1 minute before being slowly withdrawn from the brain. CB<sub>1</sub> *floxed* mice were injected with rAAV-CAG-DIO (empty control vector), AAV-CAG-DIO-CB<sub>1</sub>, or AAV-CAG-DIO-CB<sub>1</sub>-myc to induce re-expression of the CB<sub>1</sub> receptor gene in hippocampal or striatal D<sub>1</sub>-positive cells. To generate the aforementioned rAAVs, mouse CB<sub>1</sub> receptor coding sequence (either native or fused to myc-tag at the C term) was cloned in rAAV-CAG-DIO vector using standard molecular cloning technology. The coding sequence was cloned inverted in orientation to allow Cre-dependent expression of CB<sub>1</sub> receptors ([Atasoy et al., 2008](#)). In another experiment, and using the same procedure as described as above, D<sub>1</sub>-CB<sub>1</sub>-WT and D<sub>1</sub>-CB<sub>1</sub>-KO mice were injected intra hippocampally (AP  $-1.8$ ; ML  $\pm 1$ ; DV  $-2.0$  and  $-1.5$ ), with pAAV-hSyn-DIO-hM4D(Gi)-mCherry or pAAV-hSyn-DIO-mCherry (addgene, USA). For anatomical experiments and using the same procedure as above, D<sub>1</sub>-Cre and D<sub>1</sub>-CB<sub>1</sub>-KO were injected intra hippocampally with pAAV-hSyn-DIO-mCherry. In this specific experiment, expression was allowed to take place for 2 weeks. For the remaining experiments, animals were used around 4–5 weeks after local infusions. Mice were weighed daily and individuals that failed to regain the pre-surgery body weight were excluded from the following experiments.

### **Immunohistochemistry on free-floating sections**

Mice were anesthetized with pentobarbital (Exagon, Axience SAS, 400 mg/kg body weight), transcardially perfused with phosphate-buffered solution (PBS 0.1M, pH 7.4) before being fixed with 4% formaldehyde (Sigma-Aldrich). The brains were extracted and incubated overnight at  $4^\circ\text{C}$  in the same fixative, then embedded with sucrose 30% for 3 days and finally frozen in 2-methylbutane (Sigma-Aldrich) at  $-80^\circ\text{C}$ . Free-floating frozen coronal sections (40  $\mu\text{m}$ ) were cut out with a cryostat (Microm HM 500M Microm Microtech), collected in an antifreeze solution and conserved at  $-20^\circ\text{C}$ . Sections were permeabilized in a blocking solution

(in PBS: 10% donkey serum, 0.3% Triton X-100) for 1 hour at room temperature (RT). Then, sections were incubated with a rabbit primary antibody against the C-myc epitope tag (1:1000, BioLegend) overnight at 4°C. After several washes with PBS, slices were incubated for 2 hours with a secondary antibody goat anti-rabbit Alexa Fluor 488 (1:500, Fisher Scientific) and then washed in PBS at RT. Finally, sections were incubated with 4',6-diamidino-2-phenylindole (DAPI 1:20000, Fisher Scientific) diluted in PBS for 5 minutes to visualize cell nuclei and then were washed, mounted and coverslipped. All the antibodies were diluted in blocking solution. The sections were imaged with a slides scanner Hamamatsu Nanozoomer 2.0 HT.

### Combined Fluorescent *in situ* hybridization (FISH)/ Immunohistochemistry (IHC) on free-floating frozen sections

Mice were anesthetized with pentobarbital (Exagon, Axience SAS, 400 mg/kg body weight), transcardially perfused with PBS (0.1M, pH 7.4) before being fixed with 4% formaldehyde (Sigma-Aldrich). The brains were extracted and incubated overnight at 4°C in the same fixative, then embedded with sucrose 30% for 3 days and finally frozen in 2-methylbutane (Sigma-Aldrich) at –80°C. Free-floating frozen coronal sections were cut out with a cryostat (30 μm, Microm HM 500M Microm Microtech) and collected in an anti-freeze solution and conserved at –20°C.

Section were washed several times with PBS with diethyl pyrocarbonate (PBS-DEPC) to wash out the antifreeze solution. The endogenous peroxidases were inactivated by incubating the free-floating sections with 3% H<sub>2</sub>O<sub>2</sub> in PBS-DEPC for 30 minutes. All endogenous biotin, biotin receptors, and avidin binding sites present in the tissue were blocked by using the Avidin/Biotin Blocking Kit (Vector Labs, USA). Then, the slices were incubated overnight at RT with a rabbit polyclonal primary antibody against DsRed (1:1000, Takara Bio) diluted in a blocking solution (0.3% Triton X-100 diluted in PBS-DEPC). The following day, after several washes, the sections were incubated with a secondary antibody goat anti-rabbit conjugated to a horseradish peroxidase (HRP) (1:500, Cell Signaling Technology) during 2 hours at RT followed by TSA Biotin System (Biotin TSA 1:100, PerkinElmer) for 10 minutes at RT. After several washes, the slices were fixed with 4% of formaldehyde (Sigma Aldrich) for 10 minutes and blocked with 0.2M HCl for 20 minutes at RT. Then, the section were acetylated in 0.1 M Triethanolamine, 0.25% Acetic Anhydride for 10 minutes. This step was performed to reduce non-specific probe binding. Sections were hybridized overnight at 60°C with Digoxigenin (DIG)-labeled riboprobe against mouse CB<sub>1</sub> receptor (1:1000, prepared as described in [Marsicano and Lutz, 1999](#)). After hybridization, the slices were washed with different stringency wash buffers at 65°C. Then, the sections were incubated with 3% of H<sub>2</sub>O<sub>2</sub> for 30 minutes at RT and blocked 1 hour with NEN blocking buffer prepared according to the manufacturer's protocol (PerkinElmer). Anti-DIG antibody conjugated to HRP (1:2000, Roche) was applied for 2 hours at RT. The signal of CB<sub>1</sub> receptor hybridization was revealed by a TSA reaction using fluorescein isothiocyanate (FITC)-labeled tyramide (1:80 for 12 minutes, Perkin Elmer). After several washes, the free-floating slices were incubated overnight at 4°C with Streptavidin-Texas Red (1:400, PerkinElmer). Finally, the slices were incubated with DAPI (1:20000; Fisher Scientific) diluted in PBS, following by several washes, to finally be mounted, coverslipped and imaged with an epifluorescence Leica DM 6000 microscope (Leica, Germany).

## QUANTIFICATION AND STATISTICAL ANALYSIS

### Data collection

No statistical methods were used to pre-determine sample sizes, but they are similar to those reported in previous publications. All data collection and/or analysis were performed blind to the conditions of the experimenter except for the *in vivo* electrophysiological experiments. All mice were assigned randomly to the different experimental conditions.

### Fluorescence quantifications

Cells expressing mRNAs were quantified in the different layers (*stratum oriens*, *stratum pyramidale*, *stratum radiatum* and *stratum lacunosum moleculare*) of the dorsal hippocampus. CB<sub>1</sub> receptor positive cells were classified according to the level of transcript visualized by the intensity of fluorescence ([Marsicano and Lutz, 1999](#); [Terral et al., 2019](#)). “High-CB<sub>1</sub>” cells were considered to be round-shaped and intense staining covering the entire nucleus whereas “Low-CB<sub>1</sub>” cells were defined with discontinuous shape and lowest intensity of fluorescence allowing the discrimination of grains of staining.

### Statistical analyses

Data were expressed as mean ± SEM or single data points and were analyzed with Prism 6.0 (Graphpad Software), using two-tails t test (paired, unpaired) or one-way ANOVA (Dunnett's), two-way ANOVA (sidak's). Sample sizes and p values can be found in figure legends and [Table S1](#).